Variable-wavelength interferometry for optics and optoelectronics

Part 1: VAWI-1 technique

M. PLUTA

Institute of Applied Optics
ul. Kamionkowska 18, 03-805 Warszawa, Poland

In the early 1980s, a new interferometric method was devised, free from well known defects of conventional interferometry. The method is based on the use of monochromatic light, the wavelength of which is continously varied (decreased) through the visible spectrum from its red to blue regions. This method is now referred to as variable-wavelength interferometry (VAWI).

Monochromatic light of variable wavelength is commonly used in conventional interferometry to measure spectral dispersion of index of refraction [1]. Absolute distance measurements made using interferometry with variable-wavelength light have also been reported [2–4]. Light of variable wavelength was also used in reflection-contrast microscopy to determine the thickness of blood cells [5].

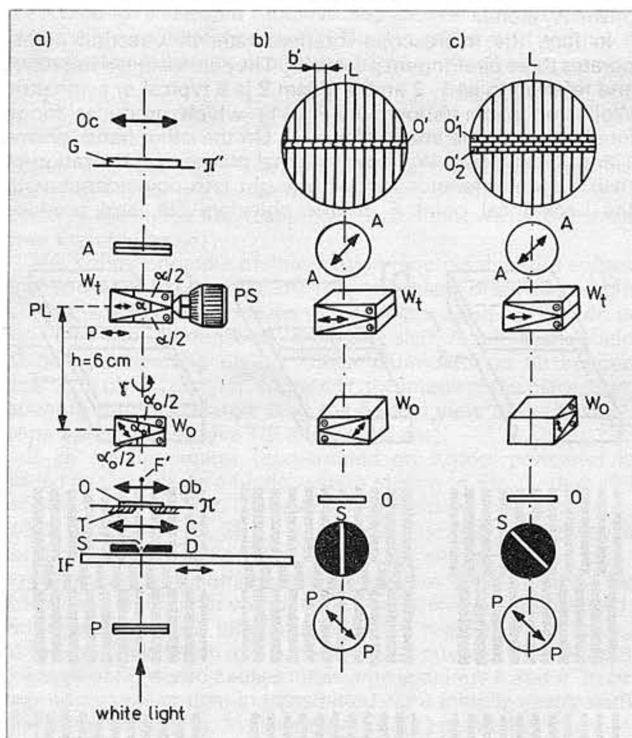

Fig. 1. Double-refracting interference system with two birefringent prisms W_o and W_t in the image space of a microscope objective *Ob*. (a) additive, (b) subtractive, (c) left-handed crossed positions of the rotatable birefringent prism W_o with respect to the transversely movable birefringent prism W_t; the latter is referred to as the tube double-refracting prism, and the former is called the objective prism. *P* – polarizer, *IF* – linear variable interference filter, *D* – slit diaphragm, *S* – slit whose width is variable, *C* – condenser, *T* – stage, *Π* – object plane, *O* – object under study, *Ob* – microscope objective, *F'* – back focal point of the objective *Ob*, *PS* – micrometric screw referred to as the phase screw, *PL* – plane of localization of own interference fringes of the prism W_o, *A* – analyzer, *Π'* – image plane of the objective *Ob*, *Oc* – ocular, *G* – its focal plate with a pointer line *L* (see text for futher explanation)

The VAWI method, covered in this article, was originally reported in a conference communication [6] in 1983 and put into practice several years later [7–24].

Initially, the VAWI method was qualified as an addition to conventional interferometric techniques to determine the integer number of interference fringes displaced by the object under study. Such a qualification was caused by interferometrically troublesome situations in which no continous connection of displaced fringes with undisplaced or reference fringes of the same interference order are observed in easily resolvable way. This method, however, was then refined and transformed into an independent, versatile interferometric procedure. Its several specific versions were described in a series of ten papers, which appeared recently (1985–1991) in Optica Acta. However, the circulation of this journal was (and still is) rather limited and the VAWI method is not widely known.

This article covers the VAWI method in a concise form and points out how it may be used in optics and/or optoelectronics to measure optical path differences and derivative quantities (e.g. thickness, refractive index and its spectral dispersion, and birefringence of solid and liquid objects). The article is divided into three parts. Each part covers one of the main techniques of the VAWI method, referred to as VAWI-1, VAWI-2 and VAWI-3.

While the VAWI method appears to be universal, the double-refracting wavefront shear interferometric systems turn out to be especially suitable for this method. A specific system of this type with variable wavefront shear was devised by the author more than 25 years ago [25–27]. The system was patented in Poland [28], the United States, Japan, the United Kingdom, Germany and ten other countries. It was used as the basis for the design of a commercial polarization interference (PI) microscope which was, and still is, mass-produced by the Polish Optical Works (PZO), Warszawa. Its short name was originally MPI-5, but since the 1970s it has been known as Biolar PI. In microscope literature, these two versions of the same instrument are also known as the Pluta interference microscope (see, e.g. Refs. [29–32]). This instrument has recently been adapted to the VAWI method as described in this article.

For the sake of completness, representative characteristics of the above mentioned double-refracting interference system is given below.

1. Double-refracting interferometric system with variable wavefront shear

The double-refracting interference system mentioned above includes a combination of two birefringent prisms W_o and W_t (Fig. 1) in the image space of a microscope objective *Ob* preceded by condenser *C*, subcondenser slit diaphragm *D* and polarizer *P*, and followed by the analyzer *A* and oculaar *Oc*. When adapted to the VAWI method, this system additionally incorporates a linear variable interference filter *IF*, which extracts monochromatic light from a source of white light (a 12 V, 100 W tungsten halogen lamp). Because of the slit diaphragm *D*, the *IF* filter is especially suitable for the interferometric method in question. A Veril S-200 filter is used, commercially available from the Schott Glaswerke, Mainz, Germany.

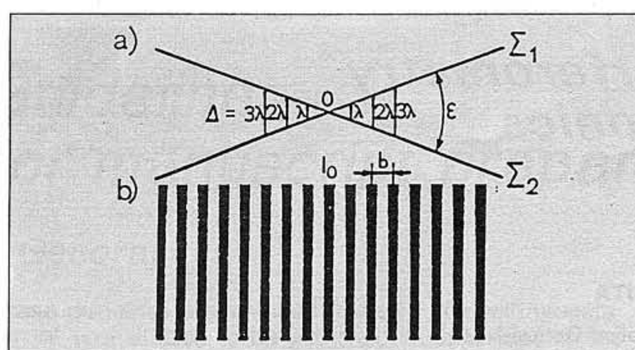

Fig. 2. Basic notation for fringe interference produced by two plane wavefronts Σ_1 and Σ_2 inclined at an angle ε to each other. Illustration of the own interference fringes of the Wollaston birefringent prism W_o (Fig. 1)

A birefringence prism W_o is installed behind and close to the rear lens of the microscope objective. The prism can be rotated about the optic axis of the objective, and is adjusted so that its own plane of localization of interference fringes is coincident with the back focal point F' of objective Ob. On the other hand, prism W_t is installed in the microscope tube at a distance of $h = 52$ to 68 mm from W_o and can be translated transversely to the objective axis by means of a precise micrometric screw, referred to as the phase screw (PS).

The translation in question is marked by the line p with arrows in Fig. 1 and causes the phase difference between two interfering wavefronts to be changed linearly. Consequently, the interference fringes produced by birefringent prism W_t and observed in image plane Π' move in the same direction p. Their interfringe spacing b (not b'!) is precisely measured with the help of the screw PS and the ocular pointer line L. The interfringe spacing b of the own interference fringes of a typical or symmetric Wollaston prism (shown in Fig. 1) is given by

$$b = \frac{\lambda}{\varepsilon} = \frac{\lambda}{2\,(n_e - n_o)\tan\alpha} \tag{1}$$

where λ is the light wavelength, $n_e - n_o = D$ is the birefringence of a double-refracting crystal (here quartz) of which a Wollaston prism is made, α is the apex angle of the prism, and

$$\varepsilon = 2\,(n_e - n_o)\tan\alpha \tag{2}$$

is the angular wavefront shear (Fig. 2), expressed in radians. On the other hand, the interfringe spacing b' observed or recorded in the image plane Π' is given by

$$b' = \frac{t_o}{h} b, \tag{3}$$

where t_o is the optical tube length of the microscope objective Ob (i.e., t_o is the distance between F' and Π') and h is the distance between the focal point F' and the plane PL of the localization of interference fringes of the Wollaston prism W_t (refer to [34] for details).

The birefringent prism W_o has an external plane of localization of its own interference fringes, which are brought into coincidence with the back focal plane of the objective Ob. Consequently, the distance h for this prism is equal to zero, and from Eq. (3) it follows that b' is equal to infinity. This means the prism W_t produces no fringes in image plane Π', but a uniform-field interference, and only Wollaston prism W is responsible for the interference fringes in this plane as shown to the right of Fig. 1. When rotated about the optic axis of the objective Ob, birefringent prism W_o enables the amount and direction of the resultant wavefront shear or image duplication to be changed. Five privileged positions of this prism are possible with respect to prism W_t: i) additive shown in Fig 1a, ii) left-handed crossed (shown in Fig. 1c; rotation angle $\gamma = 90°$, starting from additive position), iii) right-handed crossed ($\gamma = 270°$ or $-90°$), iv) subtractive (shown in Fig. 1b, $\gamma = 180°$), and v) four neutral positions ($\gamma = 45°$, 135°, 225°, and 315°). For the first (additive) position, the resultant wavefront shear (image duplication) d' in the image plane Π' is simply given by

$$d' = d'_o + d'_t \tag{4}$$

where d'_o and d'_t are the individual wavefront shears produced by the birefringent prisms W_o and W_t, respectively. It can readily be found [27, 35] that

$$d'_o = t_o \varepsilon_o$$

and that

$$d'_t = (t_o - h)\,\varepsilon.$$

It is useful for d'_o to be slightly greater or smaller than d'_t to produce a very small resultant image duplication d', i.e.

$$d' = d'_o - d'_t \approx 0 \tag{5}$$

when the birefringent prism W_o is oriented subtractively with respect to W_t as shown in Fig. 1b. Such a situation is necessary for differential fringe interferometry to measure, for instance, the birefringence of polymer textile fibers or of other birefringent objects (O, Fig. 1b) oriented diagonally with respect to axes PP and AA of polarizer P and analyzer A.

The crossed positions (left-handed and right-handed) of birefringent prism W_o lead to the resultant wavefront shear

$$d' = \sqrt{d'^2_o + d'^2_t}\,. \tag{6}$$

These are the most useful positions for microinterferometry because they produce two images (O'_1 and O'_2, Fig. 1c) of a fiber (O), an extended narrow strip or groove (Figs. 3b and 3c) and other lengthwise extended objects when they are oriented at right angles to the interference fringes produced by birefringent prism W_t in the image plane Π' (Fig. 1). If the object width is smaller than d'_o/M, where M is the magnifying power of the microscope objective Ob, the two images produced are fully separated from each other.

The neutral positions of birefringent prism W_o are much less useful than those mentioned above and do not apply to birefringent objects. In this case, the prism does not work, and the resultant wavefront shear is simply equal to d'_t produced by prism W_t alone.

In fact, the microscope interferometer in question incorporates three birefringent prisms W_t. They are installed in a turret and referred to as 1, 2 and 3. Prism 2 is a typical or symmetric Wollaston prism (shown in Fig. 1) which produces fringe interference in the image plane Π'. On the other hand, prisms 1 and 3, like prism W_o, have external planes of localization of their own interference fringes brought into coincidence with the back focal point F' of the objective Ob, and produce

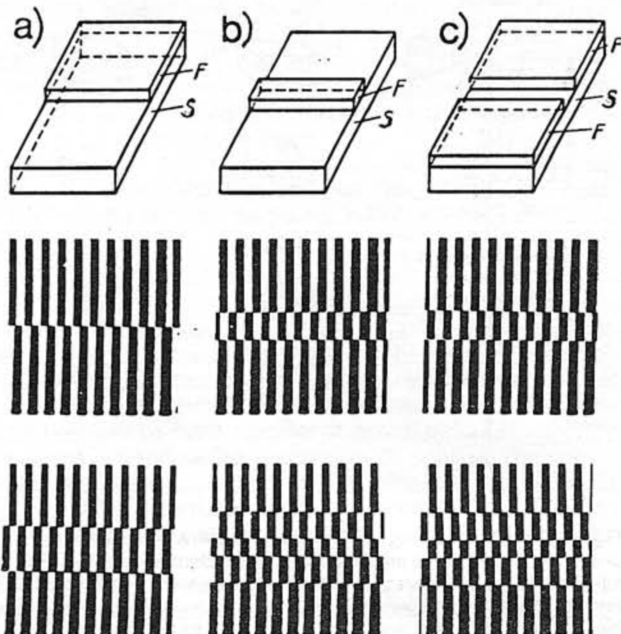

Fig. 3. Typical samples for interferometry of plate or plate-like objects, their conventional interferograms (middle rank), and wavefront shear inteferograms (bottom rank) produced by the double-refracting microscope interferometer (Fig. 1) whose objective birefringent prism W_o is crossed with the tube birefringent prism W_t (Fig 1c). (a) straight edge or half-plane object F on a plate-like substrate S, (b) extended strip object, (c) channel object

uniform-field interference in image plane Π'. Interference of this kind also applies to the VAWI method [8], but we will not discuss this problem here; only fringefield interferometry is taken into consideration in this introductory chapter. Thus, birefringent prism W_t 2 will be used as shown in Fig. 1. The angular wavefront shear ε produced by this prism is given by Eq. (2), and the angular wavefront shear initiated by prism W_o is expressed by

$$\varepsilon_o = \frac{3}{2}(n_e - n_o)\tan\alpha_o \tag{7}$$

To obtain $\varepsilon \approx \varepsilon_o$, the apex angle α of prism W is related to the α_o of prism W_o as follows

$$\tan\alpha \approx \frac{3}{4}\tan\alpha_o \tag{8}$$

or $\alpha \approx 3\alpha_o/4$. When using 10x, 20x, 40x and 100x (oil immersion) microscope objectives the apex angle α_o of birefringent prism W_o is equal to about 12°. Thus, α of a prism W_t approaches 9°.

Subcondenser polarizer P and subocular analyzer A are crossed, and their directions of light vibration (axes PP and AA, Figs. 1b and 1c) form an angle of 45° with the apex edge of the birefringent prism W_t. Slit S of subcondenser diaphragm D coincides with the front focal point of condenser C and is rotatable about the optic axis of the interferometric system so that it is always oriented at right angles to the direction of the resultant wavefront shear d' produced simultaneously by the two birefringent prisms W_o and W_t. In particular, this means that slit S is parallel to the apex angle edges of prisms W_t and W_o when the latter is oriented additively (Fig. 1a), subtractively (Fig. 1b) and neutrally with respect to the former. If, however, the prism W_o is crossed with W_t, slit S does not retain its above-mentioned direction, but must be rotated by about +45° or −45° (Fig. 1c). Moreover, slit width w is variable and must be controlled and optimized for a selected (additive, subtractive, crossed, neutral) position of birefringent prism W_o. Theoretically the slit width w is given by the following expression [35]:

$$w = \frac{\lambda f_c}{4d'}M \quad \text{to} \quad \frac{\lambda f_c}{3d'}M, \tag{9}$$

where λ is the light wavelength, f_c is the focal length of condenser C, M is the magnifying power of the objective Ob, and d' is the image duplication or the resultant wavefront shear (see Eqs. (4) to (6)).

The Köhler principle of illumination requires the light source (not shown in Fig. 1) to be imaged in the plane of slit diaphragm D. This is achieved by means of a collector (also not shown in Fig. 1). The illumination principle also requires the field diaphragm opening of the Köhler illuminator to be imaged exactly in object plane Π. Moreover, the image of the diaphragm opening cannot be larger than the field of view of the microscope system (objective Ob and ocular Oc).

If an epi-illuminator (constructed on Köhler principle) is added to the interferometric system shown in Fig. 1, then the reflected-light version of the double-refracting microinterferometer is obtained [9, 36]. The twofold passage of light waves through birefringent prisms W_t and W_o allows a pupil phase-difference autocompensation to be achieved. Thus, the Köhler epi-illuminator without any slit diaphragm may be used. However, continous interference filter IF requires the opening of the aperture diaphragm to reasonably reduced. The twofold passage of light also causes interfringe spacings b and b' to be two times smaller than in transmitted-light interferometry with dia-illumination (Fig. 1). Therefore, Eq. (1) now takes the form

$$b = \frac{\lambda}{4(n_e - n_o)\tan\alpha} \tag{10}$$

In practice, such a situation is favourable and enables the same calibration plot $b(\lambda)$ to be used for both dia- and epi-interferometry.

2. Interfringe spacing and light wavelength relationship

Determining the relationship between interfringe spacing b and light wavelength λ is a basic calibration operation in interferometry. In particular, a highly accurate calibration plot $b(\lambda)$ is an extremely essential starting tool for using the WAVI method effectively and precisely. Within the visible spectrum, such a plot can be achieved in different ways [14, 22, 37] but the first one is based on the use of highly monochromatic light sources which emit waves of extremely constant and well defined lengths. Gas lasers are among such sources.

Result of an exemplary calibration process is shown in Fig. 4 (see Refs. [37, 38] for more details). Helium-cadmium, argon and helium-neon lasers were used. Distance $l = 100b$ between the interference fringes of plus and minus fiftieth order was measured by using the phase screw PS (Fig. 1) and transverse movement of birefringent prism W_t. This movement (marked by p in Fig. 1a) is accompanied by an equivalent translation of interference fringes observed in image plane Π', and the fringe centers are precisely guided onto the pointer line L (Fig. 1b) of ocular Oc. Measurement of distance $l = 100b$ leads to highly accurate values for single interfringe spacings b. An accuracy of $b = 0.01$ µm can be easily obtained with this method. This then enables the local peak wavelength of continous interference filter IF to be read [15] with a relative error as small as $\Delta\lambda/\lambda = 0.005\%$ from the calibration plot $b(\lambda)$. Once this established, calibration plot $b(\lambda)$ is valid in perpetuity for the double refracting interference system shown in Fig. 1. For quartz Wollaston prisms, the plot of Fig. 4 is almost linear over the visible spectrum and quite consistent with Eqs. (1) and (10). Its unobservable nonlinearity follows from a small spectral dispersion of birefringence of quartz crystals. In fact, however, the nonlinearity of plot $b(\lambda)$ can be estimated to be equal to 3% within the spectral range of 400 to 750 nm and only to 2% within the spectral range of 450 to 650 nm. Such a situation permits us to extrapolate readily the plot $b(\lambda)$ over the visible spectrum and toward near UV and IR regions.

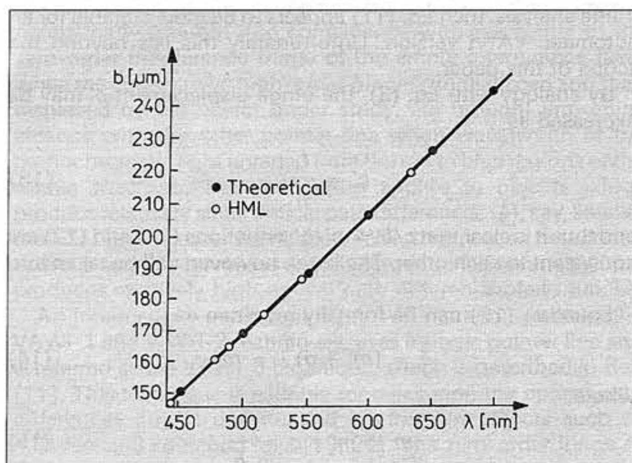

Fig. 4. Calibration plot $b(\lambda)$. The experimental values of interfringe spacing b measured in highly monochromatic light (HML) are marked by the encircled dots

It is important, however, to note that when a source of highly monochromatic (laser) light used for calibration is replaced by a source of moderately monochromatic light, say, selected from a white light source by means of conventional (metallic) interference filters, some natural limitations will arise in accurate visual interferometry within the long-wavelength (red) and short-wavelength (blue) regions of the visible spectrum [37, 38]. Namely, a tendency will appear to measure shorter and longer interfringe spacings b in the red and blue spectral regions, respectively, than those which are observed in highly monochromatic light in the same spectral regions. To overcome these limitations, a specific calibration procedure has recently been proposed [14, 22]. This new procedure uses a light source which is introduced into the double-refracting interferometer as standard equipment. The procedure depends on the use of object-adapted variable-wavelength interferometry (AVAWI). Only a birefringent quartz plate with a thickness $t = 0.65$ to 0.85 or a light-reflecting groove (step) of depth h equal to about 10 µm is required for the calibration process in dia-illumination or epi-illumination, respectively.

3. Fringe displacement expressed by interfringe spacing

Let δ be the optical path difference produced by the object under study (O, Figs. 1 and 5). In general, interferometric techniques permit us to determine δ from a simple relation

$$\delta = \frac{c'}{b'}\lambda \tag{11}$$

or

$$\delta = \frac{c}{b}\lambda \tag{12}$$

where b and b' are the interfringe spacings of the empty interference field, c and c' are the fringe displacements produced by the object, and λ is the wavelength of the monochromatic light used. The interfringe spacing b' and the fringe displacements c', however, are directly measured in the image plane Π' of the microscope interferometer by means of a micrometric ocular, e.g. filar micrometer. On the other hand, b and c are measured by using the phase micrometric screw PS (Fig. 1).

It is important to note that b' is a function of five parameters (see Eqs. (1) and (3)). These are λ, D, α, h and t_o. By contrast, b is a function of three parameters, λ, D and α. It is therefore clear that Eq. (12) is more convenient for the VAWI method than the previous one. Moreover, the calibration operation $b(\lambda)$ can be performed more accurately than $b'(\lambda)$. There are also some other limitations [34] which make Eq. (11) less useful for visual microinterferometry using the VAWI method. If, however, a CCD camera or another photoelectronic detector is used for fringe analysis, then Eq. (11) appears to be more suitable for an automatic VAWI version. Unfortunately this lies beyond the scope of this paper.

By analogy with Eq. (3), the fringe displacement c' may be expressed as

$$c' = \frac{t_o}{h}c \tag{13}$$

and thus it is clear that $c/b = c'/b'$; equations (11) and (12) are equivalent to each other. The latter, however, will be taken into account below.

Equation (12) can be formally rewritten as

$$\delta = (m_1 + q)\lambda = m\lambda \tag{14}$$

where

$$m = m_1 + q = \frac{c}{b} \tag{15}$$

is the current (generalized) interference order; m_1 is a suitably selected integer number, which will be called the initial (or introductory) interference order (if δ is smaller than λ, then $m_1 = 0$); and q is the increment (or decrement) of the current interference order m with respect to m_1. From Eq. (15) it follows that

$$(m_1 + q)\,b = mb = c. \tag{16}$$

This equation shows that the measurement of the fringe displacement c may be replaced by the more accurate measurement of the interfringe spacing b, if the initial interference order m_1 and the interference order increment q are known, observed or easily determinable. Such an approach to interferometry is possible if monochromatic light of continuously variable wavelength is used; this just applies to VAWI method.

The above relations are quite simple or even trivial, but Eq. (16) is among the fundamental equations on which the VAWI method is based.

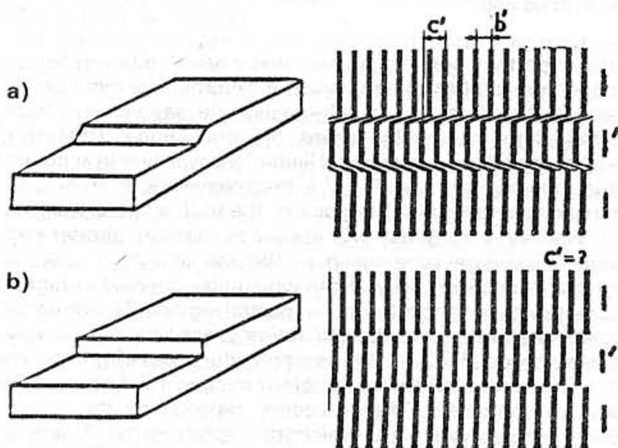

Fig. 5. Plate-like objects with (a) oblique and (b) abrupt steps and their double-refracting interference patterns. b' = interfringe spacing in the image plane Π', Fig. 1), c' = fringe displacement produced by the plate

4. Fringe movement due to continous variation of light wavelength

The interference fringe spacing varies with the light wavelength λ, which is to say that it becomes smaller as λ decreases (see Eq. (1) and Fig. 4). The variation manifests itself as the movement of the interference fringes, the higher their interference orders. Consequently, the fringes of the empty interference field (see Fig. 2b) move toward or away from the zero-order fringe I_o as λ decreases or increases, while the fringe I_o does not change its

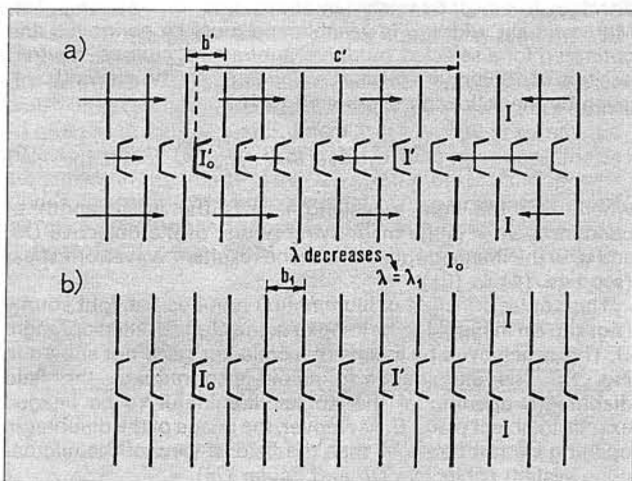

Fig. 6. Interference fringe movement due to continuous decreasing the wavelength λ of monochromatic light (diagram a), and coincident configurations of interference fringes I of the empty interference field and fringes I' displaced by an extended strip object (diagram b)

position. The latter statement is true if this fringe is completely achromatic in white light. Otherwise, some small movement of the zero-order fringe can be observed when the wavelength λ of monochromatic light is varied. Due to the small spectral birefringence of the crystalline quartz of which the double-refracting prisms W_i and W_o are made (Fig. 1), the zero-order fringe I_o (Fig. 2) is visually achromatic, but in fact it suffers from a slight chromaticity. This is not important in practice.

Now, place a step-object, such as shown in Fig. 3a, in the plane Π (Fig. 1) of the microscope interferometer in question. A near-edge zone of the step displaces the interference fringes as shown at the bottom of Fig. 3a. The same situation is schematically shown in Fig. 6, where I_o' denotes a hypothetic zero-order fringe among the interference fringes I' displaced by the step object. The fringe I_o' can be achromatic in white light only under particular conditions referred to as the object-adapted interferometry in the interfringe domain [13, 18]. For the VAWI method, however, it makes no difference which of the displaced interference fringes I' is the zero-order or achromatic fringe. Anyway,

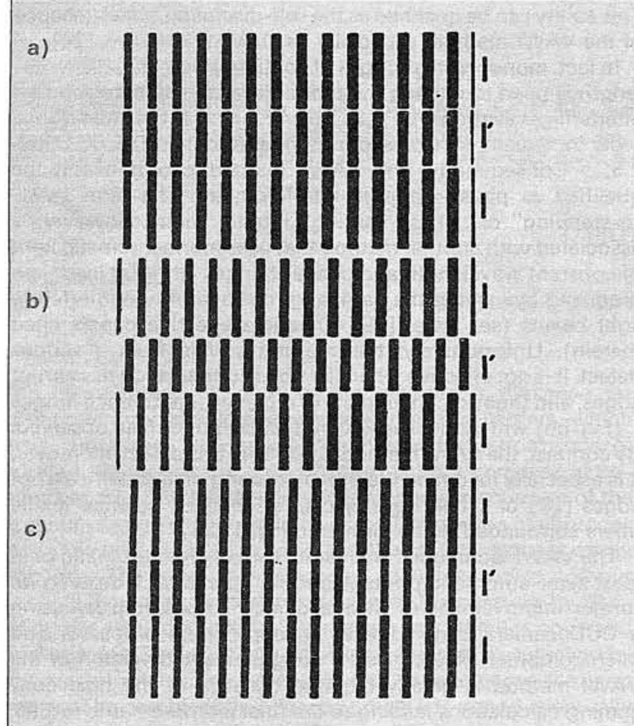

Fig. 7. Coincident (a, c) and anticoincident (b) configurations of interference fringes with decreasing light wavelength. I – reference (undisplaced) fringes, I'– fringes displaced by a straight edge of half-plane object shown in Fig. 3a

the achromatic fringe is the one which retains its constant position when the wavelength of monochromatic light is varied. It is important, however, that where the displaced achromatic fringe (or the most achromatic fringe) is found the fringes I of the empty interference field move rapidly to the zero-order fringe I_o when the wavelength λ of the monochromatic light is decreased through the visible spectrum from its red to blue regions. Similarly, the displaced fringes I' behave in a region of a fringe I_o and move quickly to their achromatic (or the most achromatic) fringe (Fig. 6a). Consequently, starting from a long wavelength permits us to select a particular wavelength λ_1 for which the displaced interference fringes I' occupy for the first time a position coincident side by side with the the reference fringes I of the empty interference field (and/or of the interference field equivalent to the empty one). Such a fringe coincidence (Fig. 6b), a single one at least within the visible spectrum, is always possible if the optical path difference δ introduced by the object to the fringe interference field is not to small, say, not smaller than λ. If, however, δ is several times greater than λ, the decreasing the light wavelength from λ_1 to λ_2, λ_3, ... causes the displaced fringes I' to be alternately anticoincident (Fig. 7b) and coincident (Fig. 7c) with the reference fringes I.

The above discussion contains the basic idea of the VAWI-1 technique. It is self-evident that the interference order increment $q = 0.5$ occurs between the first coincident (Fig. 7a) and anticoincident (Fig. 7b) configurations of the interference fringes I and I', and between the first two coincidences (Figs. 7a and c) the increment $q = 1$. The greater the optical path difference δ, the higher number of the fringe coincidences and anticoincidences over the visible spectrum.

5. Techniques and procedures specific to the VAWI method

As mentioned above, Fig. 7 expresses the principle of the VAWI-1 technique. The coincident and anticoincident configurations of interference fringes I and I' are achieved by sliding the linear variable interference filter IF (Fig. 1) and selecting particular wavelengths $\lambda_S = \lambda_1$, $\lambda_2 < \lambda_1$, $\lambda_3 < \lambda_2$, ... for which the interference fringes I', displaced by the object under study, become consecutively coincident and anticoincident side-by-side with the reference fringes (undisplaced by the object). Consequently, the interference order increments $q_S = 0, 0.5, 1, \ldots$ are fixed and observed in real time, and simultaneously the respective interfringe spacings $b_S = b_1$, $b_2 < b_1$, $b_3 < b_2$, ... are measured with the help of micrometric phase screw PS. Then the values for $\lambda_S = \lambda_1, \lambda_2, \lambda_3, \ldots$ are read out from the calibration plot $b(\lambda)$ such as shown in Fig. 4, and the optical path differences δ_1, δ_2, δ_3, ... are determined from Eq. (14). Before, however, the initial interference order m_1 must be derived from quite simple formulae:

$$m_1 = q_S \frac{\lambda_S}{\delta_{S1}\lambda_1 - \lambda_S} \tag{17}$$

or

$$m_1 = q_S \frac{b_S}{\delta_{S1} D_{1S} b_1 - b_S}, \tag{18}$$

where $\delta_{S1} = \delta_S/\delta_1$ and

$$D_{1S} = \frac{D_1}{D_S} = \frac{(n_e - n_o)_1}{(n_e - n_o)_S}. \tag{19}$$

Here as before in Eq. (1), $D = n_e - n_o$ is the birefringence of a double-refracting crystal (quartz) of which the Wollaston prism W_t (Fig. 1) is made. This technique is covered in detail by Refs. [7] and [9].

Another version of the VAWI method, the VAWI-2 technique, is covered in Refs. [10] and [12]. This uses two pointer lines whose separation is equal to about ten interfringe spacings in the red region of the visible spectrum. One of these lines is permanently brought into coincidence with the center of the zero-order interference fringe of the empty interference field, while the consecutive high-order fringes, undisplaced and then displaced by the object under study, are brought into coincidence with the other pointer line when wavelength of the monochromatic light is varied from the red to blue regions of the visible spectrum. This techniques applies to objects which produce relatively small optical path differences (δ), say, smaller than 3λ. On the other hand, the VAWI-1 technique mentioned earlier is suitable for measuring objects and their features which produces relatively high optical path differences, say, $\delta > 3\lambda$.

An intermediate version of the VAWI method, between the VAWI-1 and VAWI-2 techniques, uses a single pointer line and is referred as the VAWI-3 technique, which is described in Ref. [11]. This technique is suitable for measuring the optical path differences $\delta > 3\lambda$ of extended birefringent objects such as retarders and stretched foils [19, 20]. The zero-order fringe of the empty interference field is brought into coincidence with the pointer line, and the light wavelength is continously decreased from the red to blue regions of the visible spectrum. Simultaneously, high-order fringes displaced by the object under study are consecutively brought into coincidence with the pointer line mentioned above.

In some special circumstances, when $\delta_{S1} = 1$ and thus

$$m_1 = q_S \frac{\lambda_S}{\lambda_1 - \lambda_S} \tag{20}$$

or $\delta_{S1} D_{1S} = 1$ and then

$$m_1 = q_S \frac{b_S}{b_1 - b_S}, \tag{21}$$

the VAWI method takes a specific form, referred to as object-adapted (or adaptive) variable-wavelength interferometry (AVAWI). This enables the optical path difference or phase retardation and derived quantities (thickness, refractive index and its spectral dispersion, birefringence, etc.) to be measured very precisely using relatively simple means [13, 15, 18]. In general, the AVAWI technique enables the measuring accuracy of the optical path difference to be improved by two orders of magnitude in comparison to the conventional techniques of visual two-beam interferometry. Note that the object adaptivity

functions either in the wavelength domain ($\delta_{S1} = 1$; Eq. (20) holds good) or in the interfringe domain ($\delta_{S1} D_{1S} = 1$; Eq. (21) holds good). These two situations are denoted by AVAWI(λ) and AVAWI(b), respectively, and are covered in detail in Refs. [13] and [15] (see also [18]).

Object-adapted interferometry, however, occurs only under particular conditions, which follow from the spectral dispersion of the refractive index, birefringence, and other quantities associated with both the object under study and the interferometric optical system. In practice, the most typical interferometric situations are those which can be qualified as the quasi-object-adapted ones ($\delta_{S1} \approx 1$ or $\delta_{S1} D_{1S} \approx 1$). These are denoted by the acronym QAVAWI within the scope of the VAWI method and also use, but with some precautions, Eqs. (20) and (21) for determining the initial interference order m_1. In fact, Refs. [7]...[12] (and also Refs. [17], [19], [21], [23] and especially [24]) deal with QA variable-wavelength interferometry.

6. Advantages of the VAWI method

One of the most important advantages of the VAWI method is the fact that the only parameter that is measured directly is the interfringe spacing b, while other quantities that lead to the final interferometric results are observed, read out from the calibration plot $b(\lambda)$, and derived from quite simple formulae. Multiple interfringe spacing b_S, say, the distances $l = 20b_S$ or even $l = 40b_S$ are normally measured, giving highly accurate values for b_S. Thus, the VAWI method is much more accurate than conventional techniques of visual two-beam interferometry. In particular, the AVAWI version enables the measuring accuracy of the optical path difference to be improved by two orders of magnitude, while QAVAWI procedure offers improved accuracy of at least one order of magnitude. The accuracy of the VAWI method and related problems are discussed in detail in Ref. [15].

The majority of this article deals with both transmitted-light and reflected-light microscope interferometry of both transparent and reflecting object surrounded by an air medium. Such objects are not only suitable but even recommended for the VAWI method. The spectral dispersion of the refractive index of the air medium is very small in comparison to that of solids or liquids and can therefore be ignored at the microscopic level.

In contrast to conventional interferometry, the VAWI method is free from troubles in determining the absolute order of interference fringes displaced by the object under study as far as the optical path difference to be measured is not greater than the range of the VAWI techniques. This range is unlimited if the object-adaptivity in the interfringe domain occurs and drops to about $\delta = 30$ µm for the quasi-object-adapted version of the VAWI method [24].

It is also important to note that the VAWI method functions under specific and favourable conditions which enable the final interferometric results to be protected against operating errors.

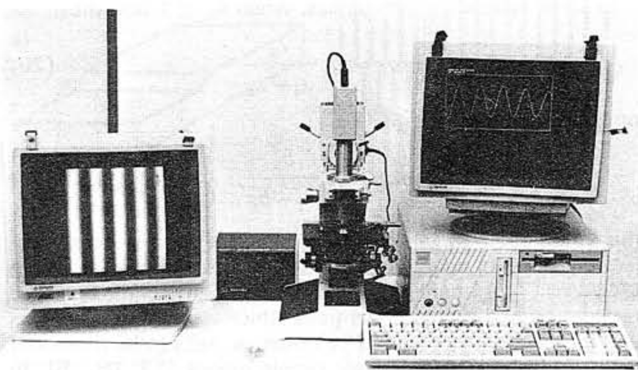

Fig. 8. Microscope interferometer MPI-10 associated with a computer and CCD camera.

This ability can be qualified as the self-discipline or self-reliance of the VAWI method, especially its QAVAWI version [24].

In fact, monochromatic light of continunously variable wavelength is used to change the phase difference ψ between two interfering wavefronts by $\pi, 2\pi, 3\pi, 4\pi, 5\pi, ...$ as the interference order increment is increased from $q_S = 0$ to $q_S = 0.5, 1, 1.5, 2, 2.5, ...$ Consequently, the VAWI method can generally be qualified as phase-stepping interferometry. The term „phase-stepping" or „phase-shifting" interferometry, however, is associated with another method that uses monochromatic light of constant wavelength and phase changes (three at least) are produced by varying the path length of one of two interfering light beams (see Refs. [39, 40] and respective papers cited therein). Unfortunately, this method suffers from a serious defect. It is not effective when the object under study has abrupt edges, and thus no connections of diplaced interference fringes I' (Fig. 5b) with undisplaced or reference fringes I are observed. By contrast, the VAWI method is free from this defect; moreover, it is especially recommended for measuring objects with abrupt edges [17] or cylindrical objects, for instance polymer textile fibers surrounded by an air medium [21, 24].

The VAWI techniques are readily suitable for automatic or at least semi-automatic photoelectronic operation. However, no further improvement of their accuracy is expected by using a CCD camera coupled with an appropriate processor and microcomputer. Neverthless, a computer-aided version of the VAWI method is greatly required because of the time consuming calculations leading to the final interferometric results.

Until now the VAWI method and its specific techniques, especially QAVAWI-1 procedure, have been applied succesfully to accurate measurement of sections, layers, thin films and other like objects (thickness, refractive index and its spectral dispersion; see [17]), birefringent retarders (phase retardation as a function of light wavelength; compare [19] and [20]), polymer textile fibers (directional refractive index $n_\parallel$ and $n_\perp$ and their spectral dispersion, birefringence and its spectral dispersion; see Ref. [21]), optical glasses (dispersion of refractive index $n(\lambda)$; refer to [23]), and other objects [8].

Finally, it is also worthwhile to note that the VAWI method has been commercially introduced into a series of new double-refracting microscope interferometers (Biolar PI 2, Biolar PI 2 dia + epi, MPI-10) designed in and available from the author's institute. Practical implementation of the VAWI method is covered by Ref. [16], and one of the above-mentioned microinterferometers is shown in Fig. 8. This illustrates the measurement of the interfringe spacing using a computer and CCD camera.

References

1. *K. Kerl*: Continuous wavelength interferometry. An effective method for measuring the dispersion of the complex index of refraction. Opt. Acta, **26** (1979) p. 1209.
2. *F. Bien, M. Camac, H.J. Caulfield* and *S. Ezekiel*: Absolute distance measurements by variable wavelength interferometry. Appl. Opt., **20** (1981) p. 400.
3. *C.W. Gillard, N. Buholz* and *D.W. Rider*: Absolute distance interferometry. Opt. Eng., **20** (1981) p. 129.
4. *V.P. Burpashov*: Application of group parameters to an using a light source with continuously variable wavelength. Avtometriya, **6** (1985) p. 91 (in Russian).
5. *J. Piper and F. Pera*: Reconstruction des Oberflachenreliefs von Erythrocyten mit Hilfe der Leitz-Reflexionskontrast Einrichtung. Leitz Sci. Tech. Inf., **7** (1980) p. 230.
6. *M. Pluta*: Identification of the interference order in interferometry by using monchromatic light with continuously variable wavelength. Abstracts of the European Optical Conference, Rydzyna, Poland 1983, p. 131.
7. *M. Pluta*: Variable wavelength interferometry. I. Fringe-field method for transmitted light. Opt. Appl., **15** (1985) p. 375.
8. *M. Pluta*: Variable wavelength interferometry. II. Uniform-field method for transmitted light. Opt. Appl., **16** (1986) p. 141.
9. *M. Pluta*: Variable wavelength interferometry. III. Reflected-light techniques. Opt. Appl., **16** (1986) p.159.
10. *M. Pluta*: Variable wavelength interferometry. IV. Alternative approach to the fringe-field method. Opt. Appl., **16** (1986) p. 301.

11. *M. Pluta*: Variable wavelength interferometry. V. Application to birefringent objects. Opt. Appl., **17** (1987) p. 47.
12. *M. Pluta*: Variable wavelength interferometry. VI. Some useful modification of the VAWI-2 technique. Opt. Appl., **17** (1987) p. 141.
13. *M. Pluta*: Variable wavelength interferometry. VII. Object-adapted method. Opt. Appl., **18** (1988), p. 75.
14. *M. Pluta*: Variable wavelength interferometry. VIII. Calibration. Opt. Appl., **20** (1990) p. 259.
15. *M. Pluta*: Variable wavelength interferometry. IX. Accuracy. Opt. Appl., **21** (1991), in press.
16. *M. Pluta*: Variable wavelength interferometry. X. Instrumentation. Opt. Appl., **21** (1991), in press.
17. *M. Pluta*: Variable wavelength interferometry of sections, lavers, thin films, and other like objects. J. Microsc., **145** (1987) p. 191.
18. *M. Pluta*: Object-adapted variable wavelength interferometry. I. Theoretical basis. J. Opt. Soc. Am., **A4** (1987) p. 2107.
19. *M. Pluta*: Variable wavelength interferometry of birefringent retarders. Opt. Laser Technol., **19** (1987) p. 131.
20. *M. Pluta*: Adaptive variable wavelength interferometry of birefringent retarders. Opt. Laser Technol., **20** (1988) p. 81.
21. *M. Pluta*: Adaptive variable wavelength microinterderometry of textile fibers. J. Microsc., **149** (1988) p. 97.
22. *M. Pluta*: Simple and accurate method of calibration of double-refracting microinterferometers using object-adapted interferometry. Interferometry '89: 100 years after Michelson: State of the Art and Applications, Z. Jaroszewicz and M. Pluta, eds., Proc. SPIE, **1121** (1990) p. 62.
23. *M. Pluta*: Variable wavelength double-refracting microinterferometry. Laser Interferometry IV: Computer-Aided Interferometry, R. J. Pryputniewicz, ed., Proc. SPIE, **1553** (in press).
24. *M. Pluta*: Quasi-object-adapted variable-wavelength double-refracting microscope interferometry. Opt. Eng., **31** (1992).
25. *M. Pluta*: Polaryzation interference microscope with variable wavefront shear. Pomiary Autom. Kontrola, **11** (1965) p. 78.
26. *M. Pluta*: A double-refracting interference microscope with variable image duplication and half-shade eyepiece. J. Phys. E (Sci. Instrum.), **2** (1969) p. 685.
27. *M. Pluta*: A double-refracting interference microscope with continuously variable amount and direction of wavefront shear. Opt. Acta, **18** (1971) p. 661.
28. *M. Pluta*: Interference-polarizing microscope. Patent No. 53149 (1963).
29. *H. Beyer* (ed): Handbuch der Mikroskopie. VEB Verlag Technik, Berlin 1973.
30. *H. Bayer*: Theorie und Praxis der Interferenzmikroskopie. Akademische Verlagsgesellschaft, Geest und Portig K.-G., Leipzig 1974.
31. *G. Goke*: Moderne Methoden der Lichtmikroskopie. Kosmos Gesellschaft der Naturfreunde Franckh'sche Verlagshandlung, Stuttgart 1988.
32. *N. Barakat and A.A. Hamza*: Interferometry of Fibrous Materials. Adam Hilger IOP Publishing Ltd., Bristol 1990.
33. *M. Francon and S. Mallick*: Polarization Interferometers. Wiley-Interscience, London 1971.
34. *M. Pluta*: On double-refracting microinterferometers which suffer from a variable interfringe spacing across the image plane. J. Microsc., **46** (1987) p. 41.
35. *M. Pluta*: Advanced Light Microscopy, Vol. 2: Specialized Methods. Elsevier, Amsterdam and PWN-Polish Scientific Publishers, Warszawa 1989, p. 157.
36. *M. Pluta*: Incident-light double-refracting interference microscope with variable wavefront shear. Opt. Acta, **20** (1973) p. 625.
37. *M. Pluta*: Relation between the peak wavelength of moderately monochromatic light and the interfringe spacing in interference patterns. I. Double refracting interference system Opt. Appl., **12** (1982) p. 19.
38. *M. Pluta*: An improved procedure for visual microinterferometry in moderately monochromatic light. Opt. Appl., **15** (1985) p. 45.
39. *M. Kujawinska*: Automatic Fringe Pattern Analysis in Optical Methods of Testing. Warsaw University of Technology Publications, Warsaw (1990).
40. *H.J. Tiziani*: Tutorial Review: Optical methods for precision measurements. Optical Quantum Electron., **21** (1989) p. 253.
41. *M. Pluta*: Birefringence of aramid fiber. Polym. Commun., **33** (1992).